2014

Spatiotemporal analysis of vegetation variability and its relationship with climate change in China

Bingwen Qiu
Fuzhou University, qiubingwen@fzu.edu.cn

Weijiao Li
Fuzhou University

Ming Zhong
Fuzhou University

Zhenghong Tang
University of Nebraska - Lincoln, ztang2@unl.edu

Chongcheng Chen
Fuzhou University

Geo-spatial Information Science, 2014
Vol. 17, No. 3, 170–180, http://dx.doi.org/10.1080/10095020.2014.959095

Taylor & Francis
Taylor & Francis Group

Spatiotemporal analysis of vegetation variability and its relationship with climate change in China

Bingwen QIU[a]*, Weijiao LI[a], Ming ZHONG[a], Zhenghong TANG[b] and Chongcheng CHEN[a]

[a]*National Engineering Research Centre of Geospatial Information Technology, Key Laboratory of Spatial Data Mining and Information Sharing of Ministry of Education, Fuzhou University, Fuzhou 350002, Fujian, China;* [b]*Community and Regional Planning Program, University of Nebraska-Lincoln, Lincoln, NE, USA*

(*Received 26 June 2013; final version received 11 July 2014*)

This paper investigated spatiotemporal dynamic pattern of vegetation, climate factor, and their complex relationships from seasonal to inter-annual scale in China during the period 1982–1998 through wavelet transform method based on GIMMS data-sets. First, most vegetation canopies demonstrated obvious seasonality, increasing with latitudinal gradient. Second, obvious dynamic trends were observed in both vegetation and climate change, especially the positive trends. Over 70% areas were observed with obvious vegetation greening up, with vegetation degradation principally in the Pearl River Delta, Yangtze River Delta, and desert. Overall warming trend was observed across the whole country (>98% area), stronger in Northern China. Although over half of area (58.2%) obtained increasing rainfall trend, around a quarter of area (24.5%), especially the Central China and most northern portion of China, exhibited significantly negative rainfall trend. Third, significantly positive normalized difference vegetation index (NDVI)–climate relationship was generally observed on the de-noised time series in most vegetated regions, corresponding to their synchronous stronger seasonal pattern. Finally, at inter-annual level, the NDVI–climate relationship differed with climatic regions and their long-term trends: in humid regions, positive coefficients were observed except in regions with vegetation degradation; in arid, semiarid, and semihumid regions, positive relationships would be examined on the condition that increasing rainfall could compensate the increasing water requirement along with increasing temperature. This study provided valuable insights into the long-term vegetation–climate relationship in China with consideration of their spatiotemporal variability and overall trend in the global change process.

Keywords: vegetation variability; wavelet transform; climate change; non-stationary; normalized difference vegetation index (NDVI)

1. Introduction

The spatiotemporal patterns of vegetation were permanently changing due to the climatic and anthropogenic causes. Determining the extent to which climate change will have influence on ecosystem processes demands long-term spatiotemporal monitoring of climate variability and its ecosystem response. Although some studies have been conducted in this field based on vegetation indices (VI) time series data-sets, more studies are needed to further investigate their complex relationships varying with spatial, temporal scales and climate regions (*1–5*). Additionally, VI time series were usually non-stationary, i.e. they present different frequency components, such as seasonal variations, long-term and short-term fluctuations (*6*). The character of non-stationarity cannot be handled by statistical method, such as ordinary least squares, spectral analysis, and Fourier transform (FT). Wavelet transform (WT) allows for the automatic localization of periodic signals, gradual shifts and abrupt interruptions, trends and onsets of trends in time series (*7*). The WT-based methods have been revealed to be efficient in the characterization of the complex spatiotemporal variability of vegetation dynamics (*6,8–11*).

China was a key vulnerable region of climate change in the world, with various topography and climate regions, diverse ecosystems, as well as high population pressure and long-term human disturbances (*12*). A number of studies have already been conducted in China, revealing vegetation dynamic and its correlation with climate factors varying among different altitudinal, latitudinal, and longitudinal gradients and also across different seasons and ecosystems (*3,13–19*). These endeavors have improved our knowledge of climate effect on vegetation in China. For these studies on vegetation dynamics in China, the traditional statistical methods were generally adopted. Several studies took this further and applied non-stationary method on some regions such as Inner Mongolia and Qinghai-Tibetan Plateau, China (*8,15*); however, till now, few of them evaluated the spatiotemporal explicit vegetation dynamic and its driving forces with non-stationarity method across the whole country. A recent study characterized the spatiotemporal non-stationarity in vegetation dynamics in China during 2001–2011 using the MODIS enhanced vegetation index data-set (*20*). However, the specific spatiotemporal characteristic of vegetation dynamic and its connection with climate change in the late twentieth century remain unclear.

*Corresponding author. Email: qiubingwen@fzu.edu.cn

To fill this gap, this study investigated the spatiotemporal characteristics of vegetation dynamic and its complicate relationships with climatic factors at multiple temporal scales in China from 1982 to 1998 based on GIMMS data-sets. The rest of the paper is organized as follows. In Section 2, the data source and methods were introduced. In Section 3, the inter- and intra-annual dynamic pattern of vegetation, climatic factors, and their multi-scale relationships were presented and discussed. In section 4, the conclusions were provided.

2. Data sources and methods

2.1. Data source

The 8-km GIMMS data-sets that comprise radiometer (AVHRR) data during 1982–1998 were used in this paper. The GIMMS data-sets were originally processed as 15 day composites using the maximum value procedure to minimize the effects of cloud contamination, respectively (*21*). Semimonthly mean temperature and monthly precipitation data with a spatial resolution of 1 km were generated from 680 weather stations throughout the country (*22*). Annual mean temperature over the study period varies from –17.5 °C in the central Tibetan Plateau to 25.4 °C in Southern China. Annual precipitation varies from less than 50 mm in the Takelamagan Desert to above 2000 mm in Southern China. China has a very diverse topography, from zero near the coastal area in the east region to the highest peak of the world in the Tibetan Plateau. We resample the climate data-set to 8 km in accord with GIMMS normalized difference vegetation index (NDVI) images.

This paper conducted a close investigation of spatiotemporal vegetation dynamic in China for the time period 1982–1998. A detailed investigation was performed on six primary natural vegetation by a per-pixel strategy (Figure 1): (I) a deciduous temperate needle-leaved forest in Xiaoxin'anling Mountains; (II) a temperate meadow in Inner Mongolia; (III) an alpine meadow in the Tibetan Plateau; (IV) a broad-leaved subtropical forest in the Wuyi Mountains; (V) an evergreen broad-leaved tropical forest in the Yunnan province; (VI) an evergreen broad-leaved tropical forest in the Hainan province.

2.2. Method

The multi-resolution analysis (MRA) by wavelet transform successively decomposes the original signal into smaller and larger scale components of the original signals, also known as detail (*D*) and approximation (*A*) series (*20*). It has been successfully applied in characterizing vegetation dynamic based on MODIS and NOAA time series images, and detailed descriptions could be found in Refs. (*10,20,23*). Due to its smoothness of the reconstructed signal, low loss of computation, and easy complementation, the Meyer orthogonal discrete wavelet

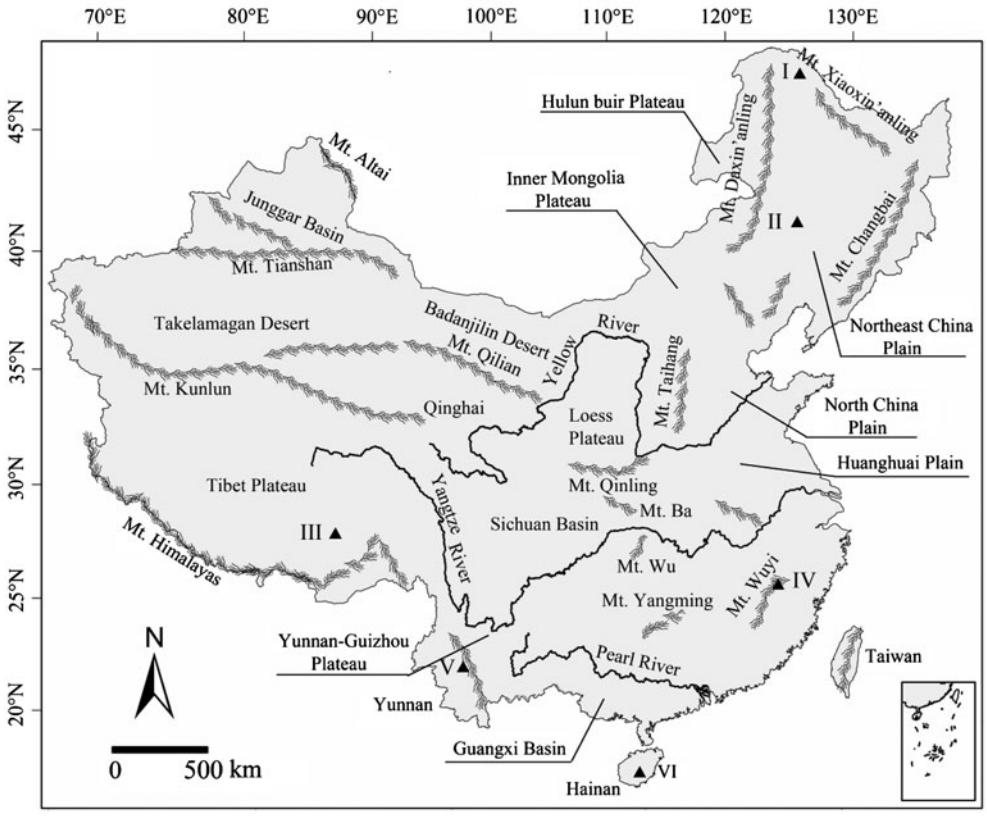

Figure 1. Location of study area.

Table 1. Period and semiperiod corresponding to the different MRA decomposition levels using the Meyer DWT and sampling period of the GIMMS and precipitation data-sets.

Level	Scale	Period of GIMMS (day)	Semiperiod of GIMMS (day)	Period of rainfall (day)	Semiperiod of rainfall (day)
1	2	45	22	89	45
2	4	89	45	178	89
3	8	178	89	357	179
4	16	357	179	714	357
5	32	714	357		

Table 2. Parameters computed from wavelet transform.

Parameter	Description
$\overline{\text{NDVI}}$	Mean of the inter-annual component $\overline{A_5}$
NDVI_{min}	Percentile 10% of the sum of mean inter-annual and intra-annual variability: $\text{NDVI}_{\text{min}} = P_{10}(\overline{A_5 + V})$
NDVI_{max}	Percentile 90% of the sum of mean inter-annual and intra-annual variability: $\text{NDVI}_{\text{max}} = P_{90}(\overline{A_5 + V})$
ΔNDVI	Range of percentiles 10% and 90% for the intra-annual variability: $\Delta\text{NDVI} = R_{10,90}(V)$
T_{max}	Timing of the maximum NDVI
T_{min}	Timing of the minimum NDVI
Q	Slope of the inter-annual component obtained from the Sen's method

was applied for this purpose (*24*). The MRA by wavelet transform was applied to the GIMMS data-sets and semi-monthly composite temperature, and monthly composite precipitation time series data-sets from 1982 to 1998.

The period and semiperiod of GIMMS and precipitation data-sets corresponding to the different decomposition scales for the Meyer wavelet were provided in Table 1 with v_c = 0.67213 and a sampling period of 15 and 30 days, respectively. Several parameters related to vegetation phenology can be obtained through MRA: $\overline{\text{NDVI}}$, NDVI_{max}, NDVI_{min}, ΔNDVI, T_{max}, T_{min}, and the trend in the data series, Q (Table 2). $\overline{\text{NDVI}}$ represents the average vegetation state during the study period. NDVI_{max} and NDVI_{min} indicate the maximum and minimum level of the NDVI. ΔNDVI denotes the amplitude of the annual phonological cycle. T_{max} and T_{min} reveal the timing of the minimum and maximum NDVI. Q, an indicator of the magnitude of total change during the study period, was calculated based on the non-parametric Sen's method (*25*). If Q was significantly different from zero, we may draw a conclusion that there exists a trend in the time series.

Pearson's product moment correlation analysis was applied to explore the relationship between NDVI and climate factors. In order to correspond to the precipitation time series data-sets, the original GIMMS NDVI data-sets were accumulated on a monthly scale. And, the relationships between wavelet components of NDVI and climate factors at different scales were explored. The moving averages of climate factors have been used to detect the relationship of these factors with vegetation dynamics (*26,27*). As climate factors change, the vegetation growth takes time to response, causing a time lag. The time lag in vegetation response to climate change has been widely observed (*28–30*); however, it differed with different climate factors and across different regions (*16,31*). To evaluate the time lag between changes in climate change and vegetation dynamics, a correlation coefficient was computed based on the corresponding month, one month moving average, and two months moving average of temperature and precipitation, respectively. For these three coefficients, the period with the strongest coefficient was found for that pixels and the time lag between NDVI and climate factors could be decided.

3. Results and discussion

3.1. *Spatiotemporal vegetation variability*

The inter- and intra-annual time series indicated by A_5 and V were computed for the six selected vegetation canopies during 1982–1998, respectively (Figure 2). Most vegetation canopies demonstrated obvious seasonality, with maximum values in summer and minimum values in winter. However, the tropical forest in the Yunnan province in Southwest China demonstrated an opposite seasonal pattern, with minimum NDVI values observed in summer season. The tropical forests in subtropical and tropical regions were observed with relatively longer growing season compared with those in temperate regions. Natural vegetation in China demonstrated obvious seasonality, stronger with latitudinal gradient as indicated by the magnitude of intra-annual component V. The inter-annual time series (A_5) distinguishes the average vegetation status during the study period. Relatively higher magnitude of inter-annual vegetation pattern was observed in the tropical and subtropical broad-leaved forest, compared with that in needle-leaved forest and meadow in temperate region. These results were generally consistent with the related study of vegetation dynamics in 2001–2011 (*20*), revealing the consistency of seasonal vegetation dynamic pattern during the past few decades.

Wavelet transform was performed on the whole image by a per-pixel strategy based on GIMMS NDVI

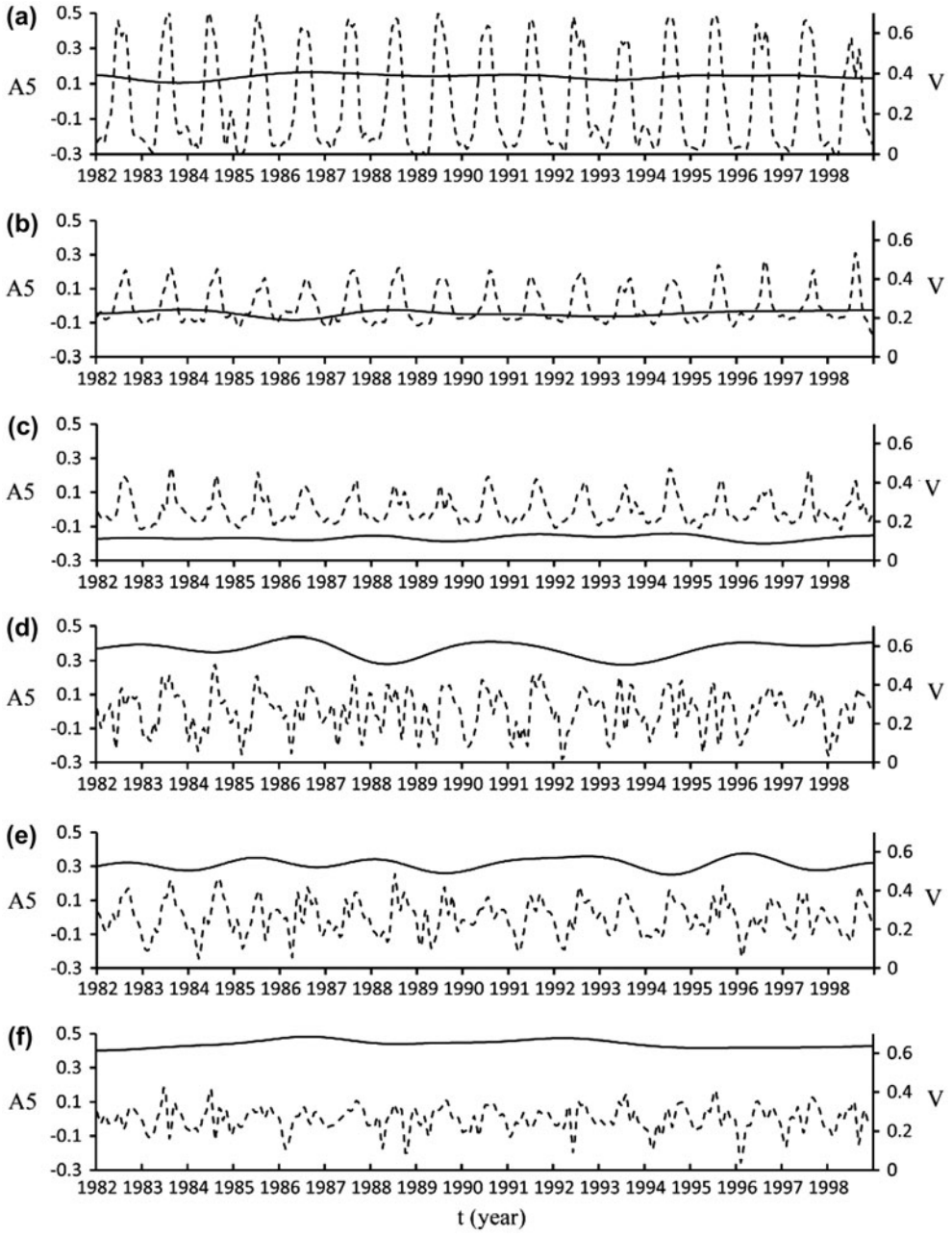

Figure 2. The intra-annual and the inter-annual component of NDVI time series for temperate forest (a), temperate meadow (b), alpine meadow (c), subtropical forest (d), tropical forest in Yunnan province (e), and in Hainan province (f).

data-sets during 1982–1998. Several key parameters representing spatiotemporal pattern of vegetation growth were derived (Figure 3). The $NDVI_{min}$ image (Figure 3(b)) provided distinct contrasted information, with maximum values in the south China and minimum values in the Northwest China. It is interesting that extremely high $NDVI_{max}$ values were examined in the Northeast China (Figure 3(a)). Very distinguished values were also observed in the ΔNDVI image (Figure 3(c)) in the North China, with extremely high values in the Northeast China and very low values (close to zero) in the Northwest China. In the East China, ΔNDVI values generally increase with latitudinal gradient.

The T_{max} image (Figure 3(d)) revealed that most pixels obtained the maximum values in August, indicating summer peaking vegetation types. The T_{min} image (Figure 3(e)) illustrated that most pixels obtained minimum values in February and March. However, exceptions were observed in the Yunnan-Guizhou Plateau, with minimum values in summer. The phenomenon was probably associated with the data quality problem, particularly the heavy cloud cover during summer season, which was confirmed in MODIS data-sets with pixel reliability (*20*).

A Q image (Figure 3(f)) based on the non-parametric Sen's method (*25*) was derived for the study area. Most pixels (70.3%) present positive trends, suggesting increasing vegetation greenness, as opposed to 12.4%

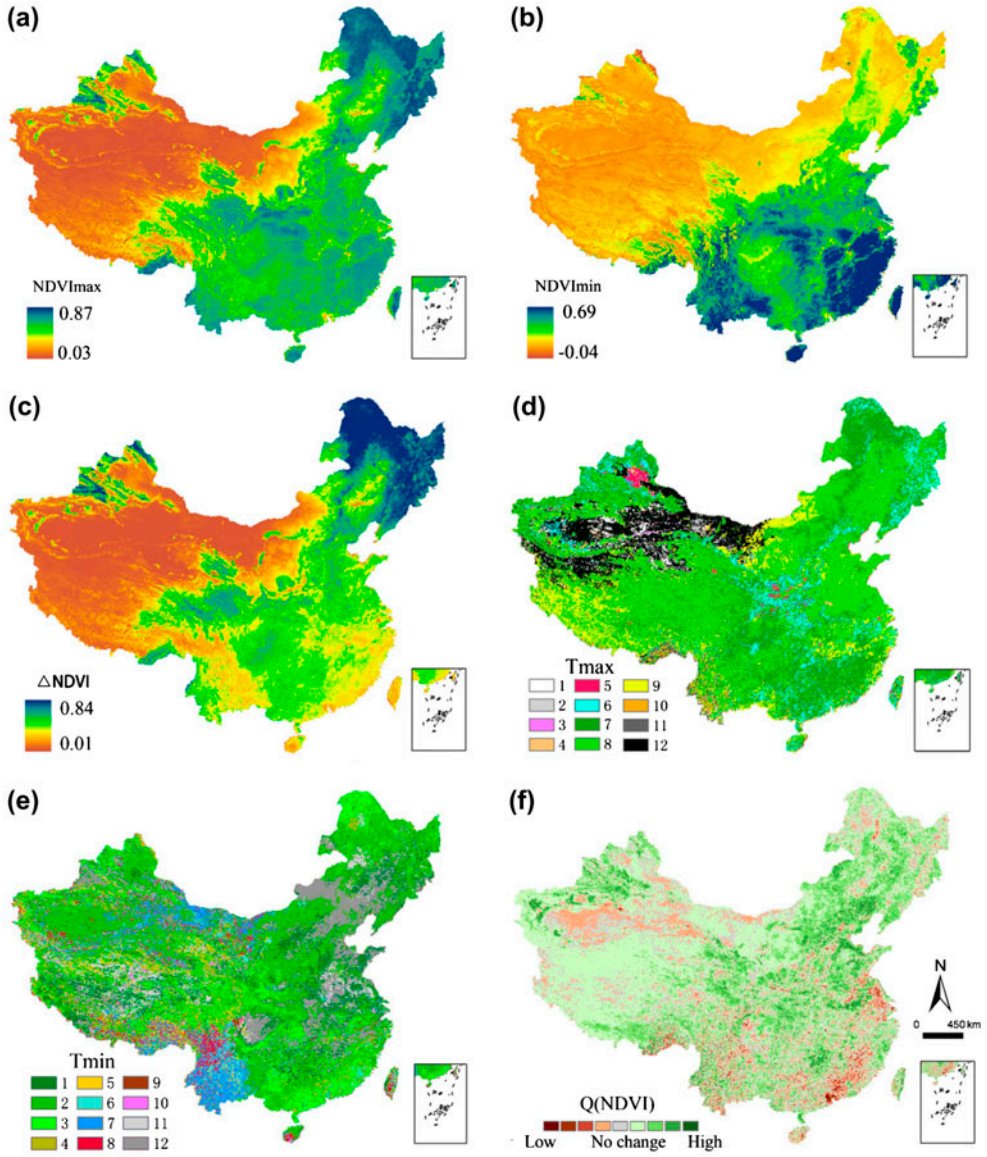

Figure 3. Spatial distribution maps of $NDVI_{max}$ (a), $NDVI_{min}$ (b), ΔNDVI (c), T_{max} (d), T_{min} (e), and Q (f).

areas of negative trends. Strong increasing vegetation trends ($Q > 0.00055$) were observed in the Northeast China, Central China, and north portion of Xinjiang province. Decreasing vegetation trends were principally examined for the desert areas, the Pearl River Delta and Yangtze River Delta. However, according to recent study, in the early twenty-first century, the northeast China experienced vegetation degradation, and the Pearl River Delta and desert regions were not examined with obvious negative trend (*20*).

3.2. *Trend analysis of temperature and precipitation*

Q images of both temperature and precipitation during 1982–1998 were derived (Figure 4). With regard to temperature, overall warming trend was observed across the whole county (over 98% area). The intensity of climate warming varies with latitude gradient: stronger increasing warming trends ($Q > 0.00025$) were observed on the North China and slightly increasing warming trends ($0 < Q < 0.00025$) were generally examined on South China and desert regions. Considering precipitation, increasing rainfall trends were observed on 58.2% pixels, especially the South China, Southwest China, and East China (Figure 4(b)). Around a quarter of area (24.5%) experienced decreasing rainfall trends, principally located in Central China, Northern Tibetan Plateau, and the north portion of Northeast China. The serious drought trends were observed in most Central China and most northern portion of China. Regions with non no obvious rainfall trends (17.3%) were generally sandwiched between them. Therefore, the South China underwent slight

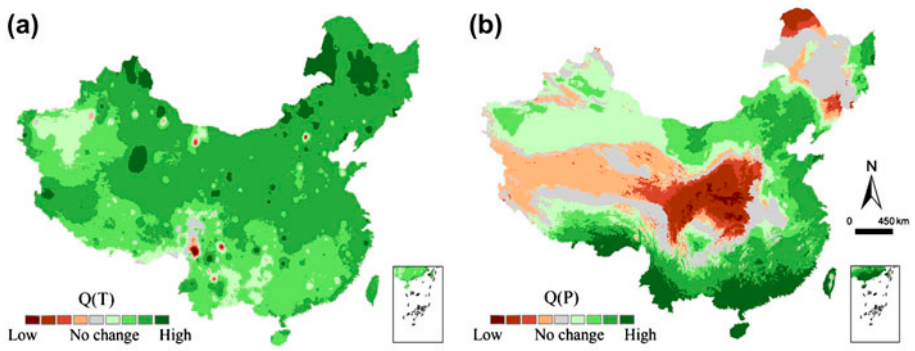

Figure 4. Slope of Q for temperature (a) and precipitation (b) derived from wavelet transform.

warming and strong increasing rainfall trend, and the Central and North China experienced strong warming and drying trends during 1982–1998.

3.3. *Spatiotemporal explicit relationships between NDVI and climate factors*

The correlation analysis was performed on the de-noised A_1, inter-annual and seasonal components of NDVI, and the temperature time series during 1982–1998, respectively. Spatial distribution images of time lag between NDVI and climate factors (temperature and precipitation) were provided in Figure 5. The time lag between NDVI and climate factors varied with different climate regions and vegetation types (Figure 5(a)). Regarding the time lag between NDVI and temperature, almost a half of the pixels (46%) were examined with 1.5–2 months' time lag, located in the West and South China. Other areas were observed with time lag of less than 1.5 months. The Yangtze River Delta and the Sichuan Basin were observed with no obvious time lag (around 18%). Considering the time lag between NDVI and precipitation (Figure 5(b)), around one-third of the pixels were examined with 2 months' time lag, mainly located in the East Tibetan Plateau and Yangtze River Delta. Another one-third of the pixels were observed with 1 month' time lag, mainly located in South China, Yunnan-Guizhou Plateau, desert areas, and north portion of Tibetan Plateau, while another one-third of the pixels with no obvious time lag were principally located in Northeast China and North China plain.

Regarding the relationship between NDVI and temperature, strong positive correlations were obtained from the de-noised A_1 time series (Figure 6(a)) in over 80% pixels. A similar spatial distribution pattern of NDVI-T relationship was obtained from the D_4 component NDVI time series, but with even stronger coefficients (Figure 6(b)). A few pixels with negative NDVI-T relationship were principally located in the Yunnan-Guizhou Plateau, Southwest China, and some deserts. At inter-annual level, although over 50% pixels were examined with positive T–NDVI relationship, only a small proportion (7%) were observed with strong coefficients (>0.7) (Figure 6(c)). Negative NDVI-T relationship at inter-annual level principally located in Inner Mongolia, Xinjiang, Yunnan-Guizhou Plateau, Tibetan Plateau, and some rapid developing regions such as the Pearl River Delta and Yangtze River Delta.

Compared with NDVI–temperature relationship, similar distribution pattern of the NDVI–precipitation coefficients at the de-noised and seasonal levels (Figure 6(e) and (f)) were observed. At inter-annual level, around one half of the pixels were examined with positive correlations (Figure 6(d)). A quarter of the pixels were observed with negative correlation at inter-annual level, mainly in Central China, Northern Tibetan Plateau,

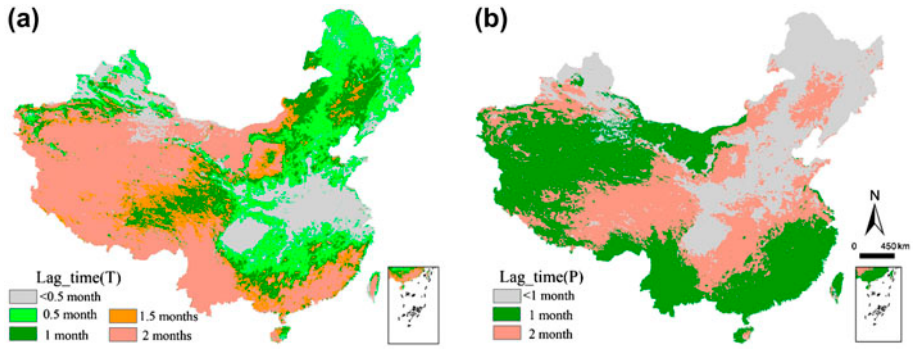

Figure 5. Spatial distribution of time lags between NDVI and temperature (a) and NDVI and precipitation (b).

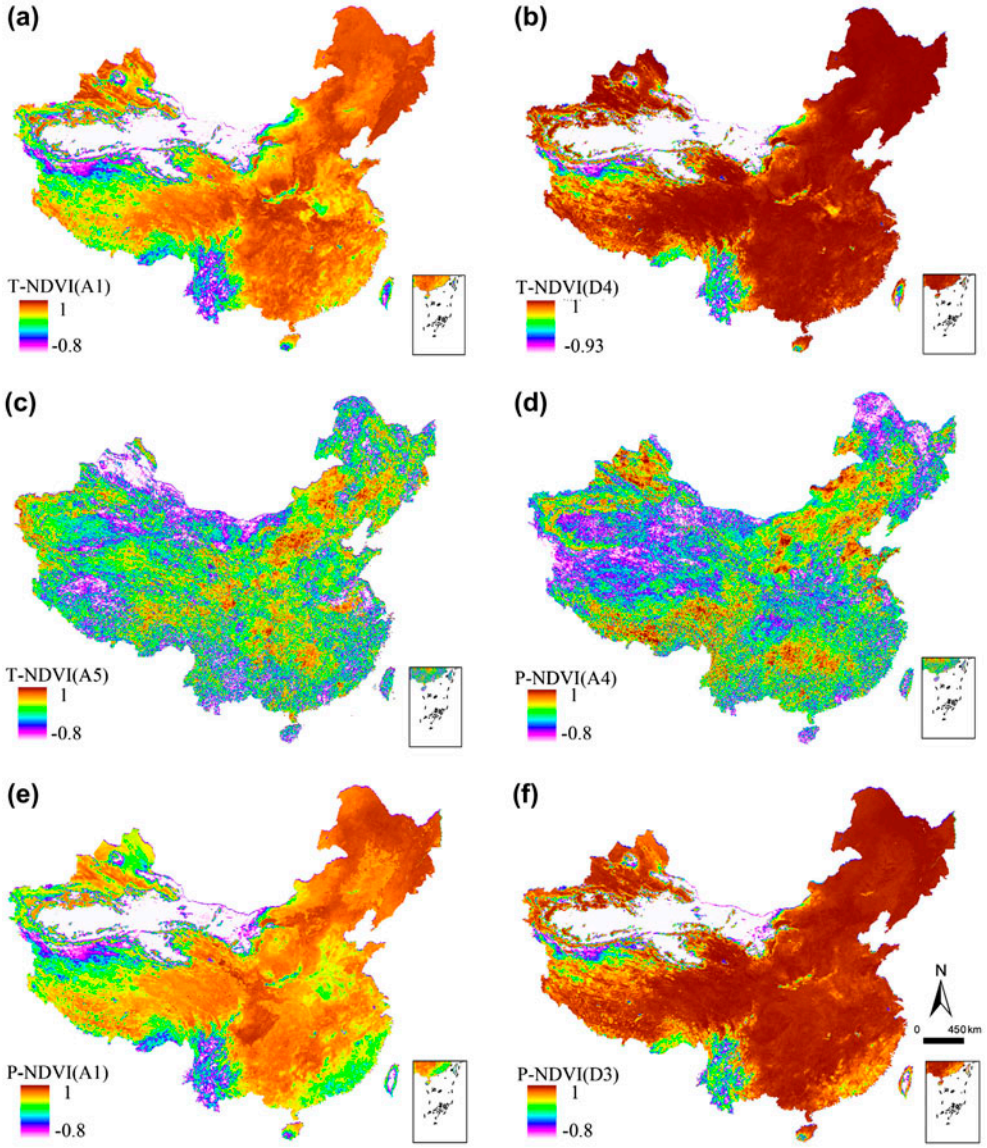

Figure 6. The spatial distribution of NDVI-climate coefficient at de-noised (a, e), inter-annual (c, d) and seasonal (b, f) scales.

Northeast China, the Pearl River Delta, and Yangtze River Delta.

Based on the combined analysis of Q and NDVI–climate coefficient images (Figures 3, 4, and 6), it seemed that the negative correlations between NDVI and climatic factors at de-noised and seasonal levels in vegetated regions were associated with data quality of GIMMS data-sets. The negative relationships at inter-annual level were connected with their negative dynamic trends. In humid regions, negative NDVI–temperature coefficients were principally located in regions with negative NDVI trends, and negative NDVI–precipitation coefficients were mainly associated with the negative dynamics trends of either NDVI or climatic factors. In arid, semi-arid, and semihumid regions, negative coefficients would be obtained when rainfall increase could not compensate the increasing water requirement with global warming.

3.4. Zoning system

Based on the above results and analysis, 10 parts were analyzed and discussed below (Figure 7).

Part A: Squeezed between Altai Mountains in the north and Tianshan Mountains in the south, part A is located in the arid region with high mountain plateau. Signals of vegetation growth were fairly strong compared with surrounding areas. Relatively strong positive vegetation trend was observed in this part, as well as a slightly positive rainfall trend and strong climate warming. This result confirms the previous research findings that a strong signal of climatic shift to warm-humid pattern has been appearing in the western part of Chinese Tianshan and Qilian Mountains since 1987 (*32*). Compared with humid region, rainfall plays a significantly role in plant growth. Vegetation has a strong positive correlation with precipitation, even at the inter-annual

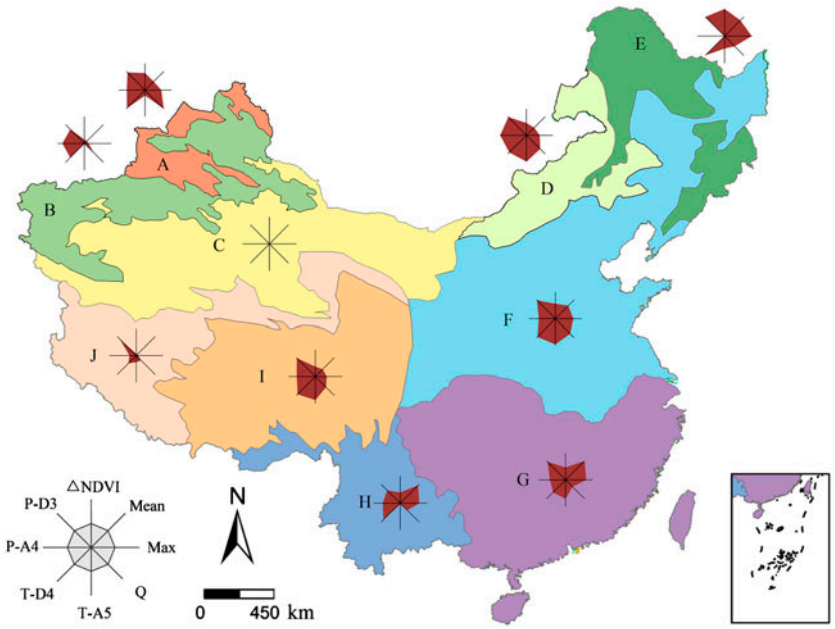

Figure 7. Zoning system of vegetation dynamic and its connection with climate factors during 1982−1998.

level. The temperature has a strong positive influence on the intra-annual vegetation variability and a slightly positive even negative effect on the long-term vegetation growth.

Part C: Located in desert region with the least annual rainfall (below 100 mm), a very slightly increasing rainfall trend as well as strongly increasing warming trend was examined. This slightly increasing precipitation could not fully complement increasing water requirements caused by temperature increase. Thus, overall decreasing vegetation trend was observed. Very weak or no signal of vegetation growth was presented, along with little connection with both temperature and precipitation.

Part B: Situated in the middle of part A and C, this part belongs to the transition type from mountain meadow to desert. Although with only slightly signal of vegetation growth in part B, relatively close relationship with climate factors could be examined. Located in the arid region, the NDVI–precipitation correlation was stronger than the NDVI–precipitation correlation at both intra-annual and inter-annual levels. With an increasing warming and rainfall trend, slightly increasing vegetation was also examined.

Part E: The most important natural forest areas in China, Daxin'anling Mountains, Xiaoxin'anling Mountains, and Changbai Mountains belong to this region. Very strong signal of plant growth cycles was observed, with the highest maximum vegetation level and seasonal patterns across the whole country. A very strong positive influence from both temperature and precipitation were examined on the intra-annual vegetation variability, which was consistent with recent study based on AVHRR and MODIS data from 1982 to 2009 (*33*). However, it seemed that precipitation generally had negative influence on the long-term vegetation growth. The negative inter-annual NDVI–precipitation coefficients needed to be further investigated, considering that the average annual precipitation is below 600 mm and there is no increasing or even a small portion of decreasing rainfall trend during 1982–1998. A large portion of this region experienced a decrease in vegetation, which was confirmed by the trend analysis. The natural forests in Northeast China suffered from deforestation as results of agricultural practices, urbanization, and fire disaster, which was also reported by related studies (*33,34*).

Part D: Located in semiarid region, the signal of vegetation growth cycle and correlation values between NDVI and climate variables generally increase from west to east, which agreed with Yang et al. study (*8*). Overall very strong climate warming pattern was examined, especially the north portion. A positive rainfall trend was also observed in the south portion, as well as a non-significant and even a negative rainfall trend in the north portion. In semiarid region, water was a prerequisite for vegetation growth. Vegetation growth has very strong positive correlation with precipitation, even at the inter-annual level. As a result, an obviously greening up was also observed in the south portion (northeast of Inner Mongolia Plateau), which was consistent with Piao et al. study (*28*). In semiarid region, the influence of temperate on vegetation growth was fairly complicate. Temperature increase might demand more water requirements for vegetation growth. With no increasing precipitation and continuing warming, only slightly increasing or even negative vegetation trend was observed in the Hulunbuir Plateau, which was also revealed by Duan et al. study (*35*).

Part F: The Taihang Mountains further separate part F into two portions: (a) the east portion with plains, including the North China Plain, Northeast China Plain, and Huanghuai Plain; (b) the west portion with plateau, principally the Loess Plateau and Ordos Plateau. Strong signal of plant growth cycles was observed in the east portion of part F, as well as much weaker vegetation growth and seasonal patterns in the west portion of part F. In the east portion of part F, very strong increasing vegetation trend was obtained, as well as distinct increasing temperature and rainfall trend. The inter-annual NDVI–climate coefficient and NDVI–precipitation coefficient were highly spatially heterogeneous. In the Loess Plateau, inter-annual NDVI variability exhibited very strong positive connection with the temperature. The long-term NDVI variability was much influenced by precipitation in North China Plain, as well as comprehensive connection with both temperature and precipitation in Northeast China Plain. The findings were consistent with related studies (*33,36,37*) and further confirmed that the inter-annual NDVI–climate relationship varied across different climate and topographic regions.

Part G: Located in a subtropical and tropical climate region, perennial good vegetation growth state was generally observed, as well as strong signal of vegetation growth cycles. The maximum NDVI was generally delayed compared with part F, examined on September and October in the coastal areas, as well as August in other interior areas. Both strongly decreasing and increasing vegetation trends were examined. Strongly decreasing vegetation trend was observed in the rapid developing regions such as the Pearl River Delta and Yangtze River Delta, which experienced rapid urbanization during the past few decades (*18,38*). Besides, decreasing vegetation was also observed in the Wuyi Mountains and Guangxi Basin, which might be related to soil erosion, land degradation, and deforesting. However, obviously greening up was also observed in China's interior forest areas such as Yangming Mountains, Qinling Mountains, and Wu Mountains. Vegetation growth in part G was strongly influenced by intensive human activities. The findings agreed with other related studies (*17,18,29,39*) and further confirmed that vegetation dynamic in subtropical and tropical climate region were controlled by the combined effect of both climate change and human activities, with short-term variability principally caused by anthropic influence.

Part H: Located in a subtropical and tropical plateau region, slightly increasing as well as decreasing vegetation trend was observed. Maximum NDVI was examined in winter season, obviously delayed compared with surrounding areas. Besides, the rarely negative intra-annual NDVI–temperature and NDVI–precipitation relationships in vegetated areas were observed, which has also been addressed in other studies (*14*). We further illustrated that it corresponds to the intra-annual variation of tropical forest, especially the abnormally minimum values regularly examined during summer period. In tropical forest regions, with saturated air humidity, the abnormal low NDVI value in summer season was possibly caused by cloud cover.

Part I and part J: Both located in alpine plateau climate zone, parts I and J belong to the semiarid and arid region, respectively. The average altitude was around 4500 m, namely the roof of the world. The signal of plant growth cycles was fairly weak (especially in part J), with delayed maximum NDVI date examined in autumn. Differed from desert region, vegetation growth generally had a close connection with temperature (part I) and precipitation (part I and J). In part I, climate factors also have strong positive influence on the long-term plant growth, which was consistent with other recent studies (*13,16*). Overall increasing temperature was observed in both parts I and J, as well as increasing rainfall observed in the south portion of part I. Suffered from the alpine plateau coldness and deficit rainfall, the plant was very sensible to both temperature and precipitation. As a result, slightly vegetation increasing trend was obtained, especially in part I.

3.5. Future work

Future work could be conducted in three aspects: (a) time series data-sets with better quality and detailed spatial and temporal resolution could be utilized. Although the 15-day composite GIMMS NDVI data-sets have been successfully applied to investigate the vegetation dynamic process, the relatively coarse resolution and data quality problem limit their further applications. The GIMMS data-sets in some regions such as the Southwest China might be seriously disturbed with cloud cover, generally with minimum NDVI values in summer season. Climatic time series data-sets with better quality corresponded to vegetation indices data-sets are also recommended. (b) Through incorporating land use change and other eco-climatological factors into the study might better account for spatiotemporal vegetation variability across the whole country in the context of ecosystem complexity. (c) As the response of vegetation growth to climate changes were nonlinear, complicate, and spatiotemporal interactive, combined modeling from micro to macro scales which can deal with the mechanistic ecosystem processes was urgently needed.

4. Conclusions

This study revealed the spatiotemporal dynamic pattern of vegetation, climate factor, and their complex relationships from seasonal to inter-annual scales across the whole country of China during the period 1982–1998 using the wavelet analysis method based on GIMMS data-sets. The following conclusions could be drawn: (a) most vegetation canopies demonstrated obvious seasonality, increasing with latitudinal gradient. (b) There existed obvious trend of both vegetation dynamic and climate change. With general vegetation greening up across the

whole country (over 70% areas), the vegetation decreasing trends were principally located in the Pearl River Delta, Yangtze River Delta, and desert. Overall warming trend was observed across the whole country, stronger in Northern China. Considering precipitation, increasing rainfall trends were observed on more than one-half areas (58.2%), and decreasing rainfall trends were obtained in Central China, Northern Tibetan Plateau, and Northeast China (24.5%). (c) Significantly, positive NDVI–climate relationships were generally observed on the de-noised time series in vegetated areas, corresponding to their synchronous stronger seasonal pattern. (d) At inter-annual level, the NDVI–climate relationship differed with climatic regions and their long-term trends: in arid and semiarid region, a strong positive relationship would be examined on the condition that increasing rainfall could compensate the increasing water requirement along with increasing temperature; in humid region, negative relationship would be observed in areas with their nonsynchronous dynamic patterns, especially vegetation degradation and decreasing rainfall trends.

Acknowledgments

The authors gratefully acknowledge the financial support received for this work from the National Natural Science Foundation of China (grant number 41071267), the Scientific Research Foundation for Returned Scholars, Ministry of Education of China (grant number [2012]940), and the Science Foundation of Fujian Province (grant numbers 2012I0005 and 2012J01167). We also would like to thank the Institute of Geographic Science and Natural Resources Research, Chinese Academy of Sciences for providing the climate data-sets.

Notes on contributors

Bingwen Qiu, PhD, an associate professor of Fuzhou University, is mainly engaged in spatial-temporal analysis and modeling of vegetation dynamics.

Weijiao Li is a graduate student of Fuzhou University.

Ming Zhong is a graduate student of Fuzhou University.

Zhenghong Tang, PhD, an associate professor, is mainly engaged in environmental planning theory and methodology.

Chongcheng Chen, PhD, professor of Fuzhou University, is mainly engaged in spatial-temporal data mining and 3D modeling.

References

(1) Raynolds, M.K.; Comiso, J.C.; Walker, D.A.; Verbyla, D. Relationship between Satellite-derived Land Surface Temperatures, Arctic Vegetation Types, and NDVI. *Remote Sens. Environ.* **2008**, *112* (4), 1884–1894.

(2) Gonzalez, P.; Neilson, R.P.; Lenihan, J.M.; Drapek, R.J. Global Patterns in the Vulnerability of Ecosystems to Vegetation Shifts due to Climate Change. *Global Ecol. Biogeogr.* **2010**, *19* (6), 755–768.

(3) Piao, S.L.; Cui, M.; Chen, A.; Wang, X.; Ciais, P.; Liu, J.; Tang, Y. Altitude and Temperature Dependence of Change in the Spring Vegetation Green-up date from 1982 to 2006 in the Qinghai-Xizang Plateau. *Agric. Forest Meteorol.* **2012**, *151* (12), 1599–1608.

(4) Dlamini, W. Probabilistic Spatio-temporal Assessment of Vegetation Vulnerability to Climate Change in Swaziland. *Global Change Biol.* **2011**, *17* (3), 1425–1441.

(5) Horion, S.; Cornet, Y.; Erpicum, M.; Tychon, B. Studying Interactions between Climate Variability and Vegetation Dynamic using a Phenology based Approach. *Int. J. Appl. Earth Obs. Geoinf.* **2013**, *20* (1), 20–32.

(6) Martínez, B.; Gilabert, M.A. Vegetation Dynamics from NDVI Time Series Analysis using the Wavelet Transform. *Remote Sens. Environ.* **2009**, *113* (9), 1823–1842.

(7) Rioul, O.; Vetterli, M. Wavelets and Signal Processing. *IEEE Signal Process Mag.* **1991**, *8* (4), 14–38.

(8) Yang, Y.; Xu, J.; Hong, Y.; Lv, G. The Dynamic of Vegetation Coverage and its Response to Climate Factors in Inner Mongolia, China. *Stochastic Environ. Res. Risk Assess.* **2012**, *26* (3), 357–373.

(9) Singh, A.; Dutta, R.; Stein, A.; Bhagat, R.M. A Wavelet-based Approach for Monitoring Plantation Crops (Tea: Camellia sinensis) in North East India. *Int. J. Remote Sens.* **2012**, *33* (16), 4982–5008.

(10) Martínez, B.; Gilabert, M.A.; García-Haro, F.J.; Faye, A.; Meliá, J. Characterizing Land Condition Variability in Ferlo, Senegal (2001–2009) using Multi-temporal 1-km Apparent Green Cover (AGC) SPOT Vegetation Data. *Global Planet. Change* **2011**, *76* (3–4), 152–165.

(11) Setiawan, Y.; Yoshino, K.; Philpot, W.D. Characterizing Temporal Vegetation Dynamics of Land Use in Regional Scale of Java Island, Indonesia. *J. Land Use Sci.* **2013**, *8* (1), 1–30.

(12) Ni, J. Impacts of Climate Change on Chinese Ecosystems: Key Vulnerable Regions and Potential Thresholds. *Reg. Environ. Change* **2011**, *11* (1), 49–64.

(13) Zhong, L.; Ma, Y.; Salama, M.S.; Su, Z. Assessment of Vegetation Dynamics and their Response to Variations in Precipitation and Temperature in the Tibetan Plateau. *Clim. Change* **2010**, *103* (3), 519–535.

(14) Wang, J.; Meng, J.J.; Cai, Y.L. Assessing Vegetation Dynamics Impacted by Climate Change in the Southwestern Karst Region of China with AVHRR NDVI and AVHRR NPP Time-series. *Environ. Geol.* **2008**, *54* (6), 1185–1195.

(15) Gao, Y.; Huang, J.; Li, S.; Li, S. Spatial Pattern of Non-stationarity and Scale-dependent Relationships between NDVI and Climatic Factors – A Case Study in Qinghai-Tibet Plateau, China. *Ecol. Indic.* **2012**, *20*, 170–176.

(16) Meng, M.; Ni, J.; Zong, M. Impacts of Changes in Climate Variability on Regional Vegetation in China: NDVI-based Analysis from 1982 to 2000. *Ecol. Res.* **2011**, *26* (2), 421–428.

(17) Peng, S.; Chen, A.; Xu, L.; Cao, C.; Fang, J.; Myneni, R.B.; Pinzon, J.E.; Tucker, C.J.; Piao, S. Recent Change of Vegetation Growth Trend in China. *Environ. Res. Lett.* **2011**, *6*, 044027.

(18) Song, Y.; Ma, M. A Statistical Analysis of the Relationship between Climatic Factors and the Normalized Difference Vegetation Index in China. *Int. J. Remote Sens.* **2011**, *32* (14), 3947–3965.

(19) Piao, S.L.; Fang, J.; Ji, W.; Guo, Q.; Ke, J.; Tao, S.; Woods, K. Variation in a Satellite-based Vegetation Index in Relation to Climate in China. *J. Veg. Sci.* **2004**, *15* (2), 219–226.

(20) Qiu, B.W.; Zeng, C.Y.; Tang, Z.H.; Chen, C.C. Characterizing Spatiotemporal Non-stationarity in Vegetation Dynamics in China using MODIS EVI Dataset. *J. Environ. Monit. Assess.* **2013**, *185* (11), 9019–9035.

(21) Brent, N.H. Characteristics of Maximum-value Composite Images from Temporal AVHRR Data. *Int. J. Remote Sens.* **1986**, *7* (11), 1417–1434.
(22) Fang, J.; Piao, S.; Tang, Z.; Peng, C.; Ji, W. Interannual Variability in Net Primary Production and Precipitation. *Science* **2001**, *293* (5536), 1723.
(23) Martínez, B.; Gilabert, M.A. Vegetation Dynamics from NDVI Time Series Analysis using the Wavelet Transform. *Remote Sens. Environ.* **2009**, *113* (9), 1823–1842.
(24) Abry, P. *Ondelettes et Turbulences. Multirésolutions, Algorithmes de Décomposition, Invariance d'Échelle et Signaux de Pression, Nouveaux Essais;* Diderot: Paris, 1997.
(25) Sen, P.K. Estimates of the Regression Coefficient Based on Kendall's Tau. *J. Am. Stat. Assoc.* **1968**, 1379–1389.
(26) Chang, C.T.; Lin, T.C.; Wang, S.F.; Vadeboncoeur, M.A. Assessing Growing Season Beginning and End Dates and their Relation to Climate in Taiwan using Satellite Data. *Int. J. Remote Sens.* **2011**, *32* (18), 5035–5058.
(27) Yu, F.; Price, K.P.; Ellis, J.; Shi, P. Response of Seasonal Vegetation Development to Climatic Variations in Eastern Central Asia. *Remote Sens. Environ.* **2003**, *87* (1), 42–54.
(28) Piao, S.L.; Mohammat, A.; Fang, J.; Cai, Q.; Feng, J. NDVI-based Increase in Growth of Temperate Grasslands and its Responses to Climate Changes in China. *Global Environ. Change* **2006**, *16* (4), 340–348.
(29) Piao, S.L.; Fang, J.Y.; Zhou, L.M.; Guo, Q.H.; Henderson, M.; Ji, W.; Li, Y.; Tao, S. Interannual Variations of Monthly and Seasonal Normalized Difference Vegetation Index (NDVI) in China from 1982 to 1999. *J. Geophys. Res.* **2003**, *108* (D14), 4401.
(30) Chapin, F.S.; Starfield, A.M. Time Lags and Novel Ecosystems in Response to Transient Climatic Change in Arctic Alaska. *Clim. Change* **1997**, *35* (4), 449–461.
(31) Bao, Y.J.; Song, G.B.; Li, Z.H.; Gao, J.X.; Lu, H.Y.; Wang, H.M.; Cheng, Y.; Xu, T. Study on the Spatial Differences and its Time Lag Effect on Climatic Factors of the Vegetation in the Longitudinal Range-Gorge Region. *Chin. Sci. Bull.* **2007**, *52*, 42–49.
(32) Shi, Y.F.; Shen, Y.; Dongliang, L.; Guowei, Z.; Yongjian, D.; Ruji, H.; Ersi, K. Discussion on the Present Climate Change from Warm-dry to Warm-wet in Northwest China. *Quat. Sci.* **2003**, *23* (2), 152–164.
(33) Mao, D.; Wang, Z.; Luo, L.; Ren, C. Integrating AVHRR and MODIS Data to Monitor NDVI Changes and their Relationships with Climatic Parameters in Northeast China. *Int. J. Appl. Earth Obs. Geoinf.* **2012**, *18*, 528–536.
(34) Liu, W.; Cai, T.; Ju, C.; Fu, G.; Yao, Y.; Cui, X. Assessing Vegetation Dynamics and their Relationships with Climatic Variability in Heilongjiang Province, Northeast China. *Environ. Earth Sci.* **2011**, *64* (8), 2013–2024.
(35) Duan, H.; Yan, C.; Tsunekawa, A.; Song, X.; Li, S.; Xie, J. Assessing Vegetation Dynamics in the Three-North Shelter Forest Region of China using AVHRR NDVI Data. *Environ. Earth Sci.* **2011**, *64* (4), 1011–1020.
(36) Hao, F.; Zhang, X.; Ouyang, W.; Skidmore, A.; Toxopeus, A. Vegetation NDVI Linked to Temperature and Precipitation in the Upper Catchments of Yellow River. *Environ. Model. Assess.* **2012**, *17* (4), 389–398.
(37) Miao, C.Y.; Yang, L.; Chen, X.H.; Gao, Y. The vegetation Cover Dynamics (1982–2006) in Different Erosion Regions of the Yellow River Basin. *China. Land Degrad. Develop.* **2012**, *23* (1), 62–71.
(38) Chen, X.L.; Zhao, H.M.; Li, P.X.; Yin, Z.Y. Remote Sensing Image-based Analysis of the Relationship Between Urban Heat Island and Land Use/cover Changes. *Remote Sens. Environ.* **2006**, *104* (2), 133–146.
(39) Sun, J.; Wang, X.; Chen, A.; Ma, Y.; Cui, M.; Piao, S. NDVI Indicated Characteristics of Vegetation Cover Change in China's Metropolises over the Last Three Decades. *Environmental Monit. Assess.* **2011**, *179* (1), 1–14.